DE LA RECHERCHE À L'INDUSTRIE

Recent advances in semi-lagrangian approach for gyrokinetic plasma turbulence simulations

V. Grandgirard[1], G. Latu[1]

Collaborations with physicists:

J. Abiteboul[2], Y. Dong[3], D. Estève[1], X. Garbet[1], J.B Girardo[1], Ph. Ghendrih[1], F. Palermo[1], Y. Sarazin[1], A. Strugarek[7], D. Zarzoso[2]

Collaborations with mathematicians:

A. Back[4], T. Cartier-Michaud[1], M. Mehrenberger[5], L. Mendoza[2], E. Sonnendrücker[2]

Collaborations with computer scientists:

J. Bigot[6], C. Passeron[1], F. Rozar[1,6], O. Thomine[1]

[1]CEA, IRFM, Cadarache, France
[2]IPP Garching, Germany
[3]LPP, Paris, France
[4]CPT, Marseille, France
[5]IRMA, Strasbourg, France
[6]Maison de la Simulation, Saclay, France
[7]Montreal university, Canada

ANR GYPSI
ANR G8-Exascale Nufuse
ADT-INRIA SELALIB
AEN-INRIA Fusion

www.cea.fr

Turbulence governs Fusion plasma performance

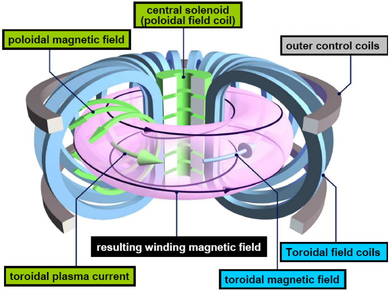

magnetic toroidal geometry (r, θ, φ)

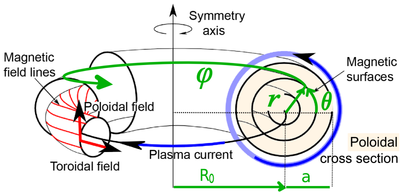

- Certainty: Turbulence limit the maximal value reachable for n and T
  - ➠ Generate loss of heat and particles
  - ➠ ↘ Confinement properties of the magnetic configuration
- Subject of utmost importance ➠ optimizing experiments like ITER and future reactors.

Gyrokinetic theory: ➠ large phase space reduction 6D to 5D

Kinetic theory: ➠ 6D distribution function of particles
(3D in space and 3D in velocity) $F_s(r, \theta, \varphi, v_\parallel, v_\perp, \alpha)$

- Fusion plasma turbulence is low frequency:

$$\omega_{\text{turb}} \sim 10^5 s^{-1} \ll \omega_{ci} \sim 10^8 s^{-1}$$

- Phase space reduction: fast gyro-motion is averaged out
  - ➠ Adiabatic invariant: magnetic momentum $\mu = m_s v_\perp^2/(2B)$
  - ➠ Velocity drifts of guiding centers

☺ Large reduction memory/CPU time

☹ Complexity of the system

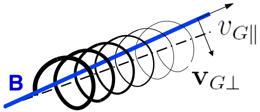

Gyrokinetic theory: ➠ 5D distribution function of guiding-centers
$\bar{F}_s(r, \theta, \varphi, v_{G\parallel}, \mu)$ where μ plays parameter role

- GK codes require state-of-the-art HPC techniques and must run efficiently on more than thousands processors.
  - non-linear 5D simulations
  - multi-scale problem in space and time
    - time: $\Delta t \approx \gamma^{-1} \sim 10^{-6}s \rightarrow t_{\text{simul}} \approx$ few $\tau_E \sim 10s$
    - space: $\rho_i \rightarrow$ machine size a $\quad \rho_* \equiv \frac{\rho_i}{a} \ll 1$

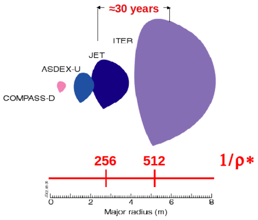

✓ ρ_* ITER $= 1/512$

✓ Number grid points $\sim (\rho_*)^{-3}$

Huge mesh for global simulations

There exist around ten 5D gyrokinetic codes for plasma fusion in the world.

- Various numerical schemes:
  - Lagrangian (PIC), Eulerian or Semi-Lagrangian
- Various simplifications:
  - δf codes: scale separation between equilibrium and perturbation.
  - Flux-tube codes ⇒ the domain considered is a vicinity of a magnetic field line.
  - Fixed gradient boundary conditions.
  - Collisionless.
- A new generation of global full-f gyrokinetic codes is being developed with collisions and flux-driven boundary conditions.
  - GYSELA (GYrokinetic SEmi-LAgrangian code) is one of them

GYSELA is a 5D non-linear gyrokinetic code used to study ion turbulence (self-organisation & control) in Tokamak plasmas.

1. GYSELA code
2. What challenges for Exascale ?
3. What challenges in terms of numeric ?
   - Modifications of the numerical scheme to improve mass and energy conservation.

GYSELA schematic view

geometry

mesh
(equidistant in (r,θ,φ))

magnetic configuration
(simplified circular concentric)

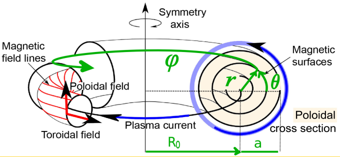

Vlasov

5D Vlasov solver for D + W
(semi-lagrangian scheme)

+

adiabatic electrons

$$B^*_{\|s}\frac{\partial \bar{F}_s}{\partial t} + \nabla\cdot\left(\frac{d\mathbf{x}_G}{dt}B^*_{\|s}\bar{F}_s\right) + \frac{\partial}{\partial v_{G\|}}\left(\frac{dv_{G\|}}{dt}B^*_{\|s}\bar{F}_s\right) = C(\bar{F}_s) + S + \mathcal{K}_{\rm buff}(\bar{F}_s) + \mathcal{D}_{\rm buff}(\bar{F}_s)$$

with the equations of motion:

$$B^*_{\|s} d_t\mathbf{x}_G = v_{G\|}\mathbf{B}^* + \frac{1}{e}\mathbf{b}\times\nabla\Lambda$$

$$B^*_{\|s} m_s d_t v_{G\|} = -\mathbf{B}^*\cdot\nabla\Lambda$$

where $\mathbf{B}^* = \mathbf{B} + (m_s v_{G\|}/e)\nabla\times\mathbf{b}$ and $\Lambda = eJ_0\phi + \mu B$;

J_0 = gyroaverage
(Padé approximation)

Poisson

3D Poisson solver (Finite Differences in r + Fourier in (θ,φ))

$$\frac{e}{T_{e,eq}}\left(\phi - \langle\phi\rangle\right) - \frac{1}{n_{e_0}}\sum_s Z_s\nabla_\perp\cdot\left(\frac{n_{s,eq}}{B\Omega_s}\nabla_\perp\phi\right) = \frac{1}{n_{e_0}}\sum_s Z_s\int J_0\cdot\left(\bar{F}_s - \bar{F}_{s,eq}\right)d^3v$$

- GYSELA is based on a Backward Semi-Lagrangian scheme (BSL)
- Solve advective form of Vlasov equation :

$$\frac{\partial f}{\partial t} + u(x)\frac{\partial f}{\partial x} = 0 \text{ with } \frac{dx}{dt} = u(x) \quad \Rightarrow \quad \frac{df}{dt} = 0$$

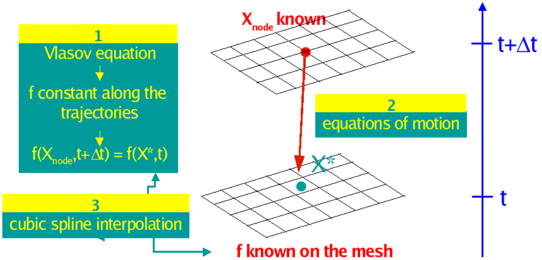

[Sonnendrücker, JoCP 1999]

- Cubic splines: A good compromise between accuracy and simplicity but their global character increase the parallelisation complexity

- Parallel decomposition example for $Nproc\_r = 3$, $Nproc\_\theta = 4$, $Nproc\_\mu = 8$

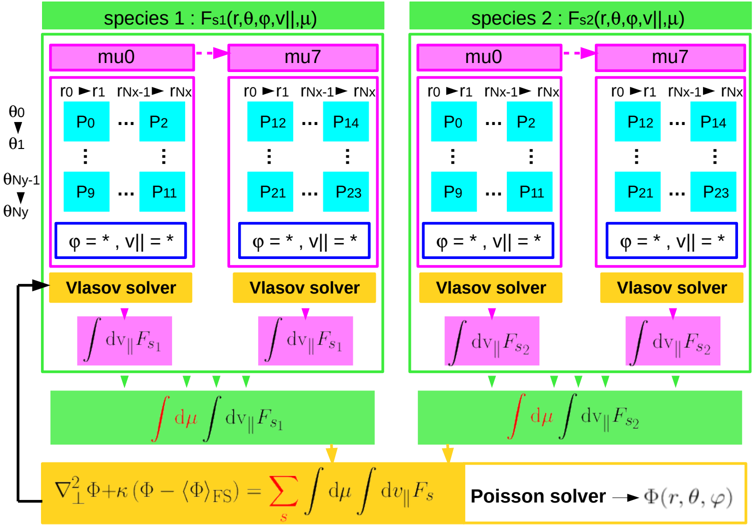

- Parallel decomposition example for $Nproc\_r = 3$, $Nproc\_\theta = 4$, $Nproc\_\mu = 8$

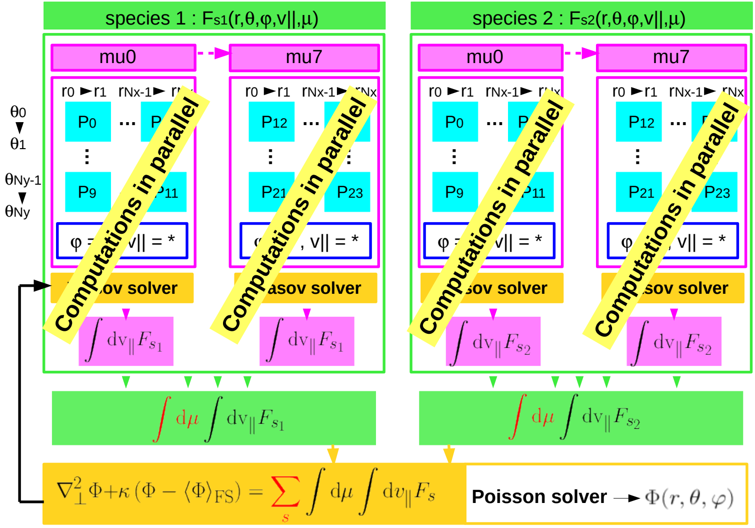

- Parallel decomposition example for $Nproc\_r = 3$, $Nproc\_\theta = 4$, $Nproc\_\mu = 8$

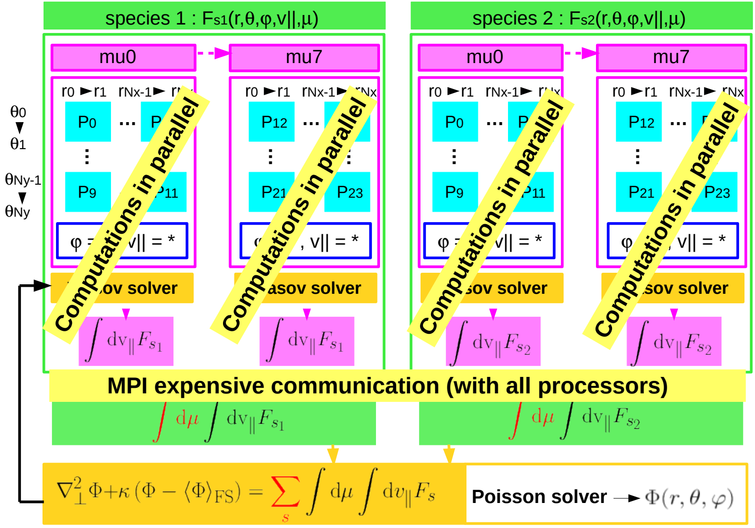

- Parallel decomposition example for $Nproc\_r = 3$, $Nproc\_\theta = 4$, $Nproc\_\mu = 8$

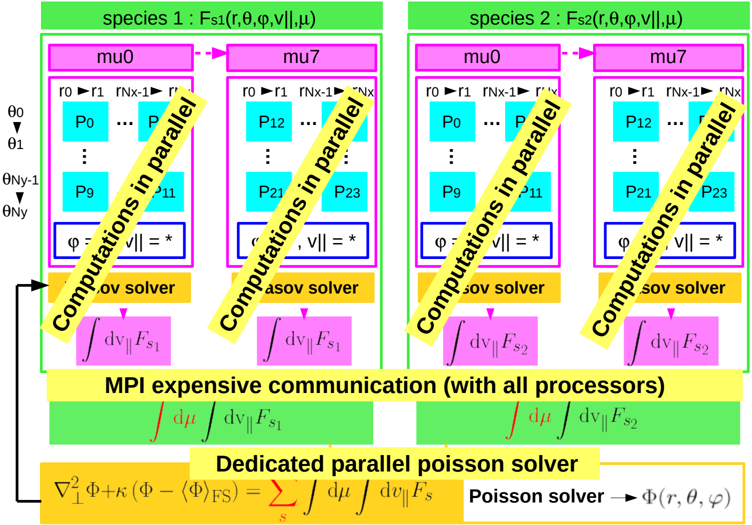

A typical run: several restarts

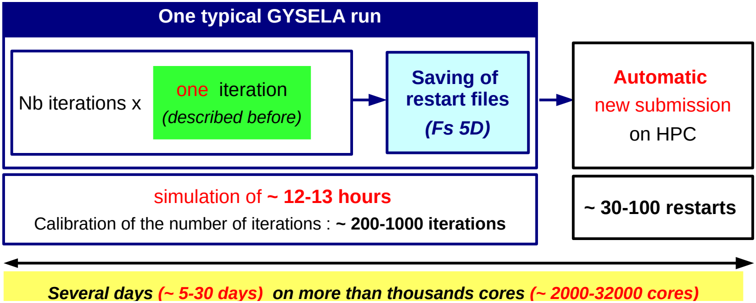

A typical run: several restarts

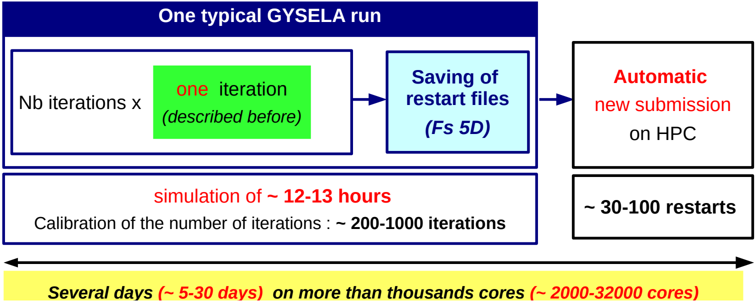

- Example of simulation in progress *[working group Comp. Simu/Exp. with LPP: O. Gurcan, P. Hennequin, P. Morel, L.Vermare]*
  - $\rho_* = 1/300$ for a quarter of torus,
  - mesh of 86 billion of points ➠ $(N_r, N_\theta, N_\varphi, N_\mu) = (512, 512, 128, 128, 20)$
  - restart files: $\sim$ 1.3 TBytes ➠ $2 \times$ (320 files of 2 GB)
  - run on 5120 cores ➠ $(\mathrm{Nproc}_r = 4, \mathrm{Nproc}_\theta = 4, \mathrm{Nproc}_\mu = 20, \mathrm{Nb}_{\mathrm{thread}} = 16)$
  - 47000 iterations already performed (1.5 million of Ω_c time $\sim$ 14.4 ms)
  - performed on IFERC machine (Rokkasho-Japan) during $\sim$ 38 days

  $\sim$ 4.8 millions of mono-processor hours *[G. Dif-Pradalier et al., TTF 2013]*

GYSELA Flux-driven simulations

- Generation & transport of toroidal rotation / Role of turbulence & boundary conditions
  - *[J. Abiteboul et al., PPCF 2013]*
- Transport barrier relaxations with E_r shear
  - *[A. Strugarek et al., PPCF 2013]*
  - *[A. Strugarek et al., PRL submitted]*
  - *[Y. Sarazin, V. Grandgirard and A. Strugarek, La Recherche, nov. 2012]*
- Interaction energetic particles & turbulence via EGAMs
  - *[D. Zarzoso et al., PRL 2013]*
- Comparison with experiments
  - *[invited G. Dif-Pradalier , TTF 2013]*

Snapshots of non-axisymmetric electric potential fluctuations

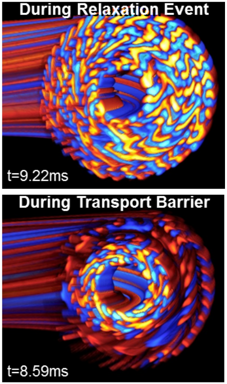

GYSELA Flux-driven simulations

- Generation & transport of toroidal rotation / Role of turbulence & boundary conditions
  - *[J. Abiteboul et al., PPCF 2013]*
  - ☹ $N = 9$ instead $N = 18$ for ripple effects
- Transport barrier relaxations with E_r shear
  - *[A. Strugarek et al., PPCF 2013]*
  - *[A. Strugarek et al., PRL submitted]*
  - *[Y. Sarazin, V. Grandgirard and A. Strugarek, La Recherche, nov. 2012]*
  - ☹ Reduced $\rho_* = \rho_i/a$: 1/150 instead of 1/500
- Interaction energetic particles & turbulence via EGAMs
  - *[D. Zarzoso et al., PRL 2013]*
  - ☹ Not possible to treat very energetic particles
- Comparison with experiments
  - *[invited G. Dif-Pradalier , TTF 2013]*
  - ☹ Several τ_E times not accessible

Snapshots of non-axisymmetric electric potential fluctuations

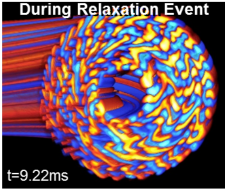

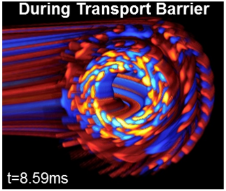

- **Work in progress with physicists:** (Not discussed here)
  - Energetic particles *[J.B Girardo (PhD)]*
  - Transport of impurities *[D. Esteve (PhD)]*
  - Spectral transfers *[Y. Dong (PhD-LPP)]*
  - Trapped electrons *[T. Cartier-Michaud (PhD)]*

  [F. Palermo (Post-Doc ANR GYPSI)]

$\Downarrow$

- **Objectives:** Always more physics to be closer and closer to experimental parameters
  - ➠ parallel optimisation of the code and development of new numerical schemes are crucial.
  - ➠ Numerical schemes are constrained by parallelisation and vice versa

Outline

1. GYSELA code
2. What challenges for Exascale ?
3. What challenges in terms of numeric ?
   - Modifications of the numerical scheme to improve mass and energy conservation.

ITER-type simulation for an energy confinement time unreacheable ➠ Exascale Needs

➠ GYSELA is already using currently Petascale machine (~ 50 million hours/year)

☹ Compromise machine size & simulation up to energy confinement time must be found

- GYSELA simulation close to ITER-like parameters : 272 billions of points
- Longest time simulation: $10^6/\Omega_c \sim 1/2$ energy confinement time

	Number of points (ρ*=ρ_i/a)	Time /Ωc	Number of cores	Number of days of simulation
Gd Challenge CINES 2010	272 billions (ρ*=1/512)	147 840	8192	31
Gd Challenge CURIE 2012	33 billions (ρ*=1/150)	678 510	16384	15
	=> Adding of Tritium		32768	4
Comparison with experiment (in progress)	87 billions (ρ*=1/512)	1 000 000	5520	23

➠ GYSELA will require Exascale machine for realistic kinetic electrons

- With electrons: $\rho_{\text{ions}}/\rho_{\text{elec}} = 60$ ➠ mesh size $\times 60^3$ and time step$/60$!!!

Some exascale bottlenecks for GYSELA

- Increase of number of cores ⇒ Hardware/Software failures more frequent

  ➠ Post-Doc ANR-Nufuse G8@Exascale: *O. Thomine (oct 2011-oct 2013)*
  ↪ Fault tolerance improvement
  ↪ Non-blocking writing of restart files *[O. Thomine et al., ESAIM proceedings 2013]*

- BlueGene Architecture fits some of the foreseen requirements for Exascale

  ➠ Post-Doc MDS/PRACE: *J. Bigot (july 2012-july 2014)*
  ↪ Adapting the code for BlueGene architecture
  [J. Bigot, F. Rozar al., ESAIM proceedings 2013]

- Memory reduction per nodes:

  ➠ PhD Maison De la Simulation / IRFM: *F. Rozar (dec 2012-dec 2015)*
  ↪ Development of dedicated tools for memory scalability
  [F. Rozar et al., accepted to PPAM2013]

- Big data ~ Several hundred TBytes: Question of transfer, storage, visualisation

  ↪ HLST support (IPP Garching) for data compression and parallel writting
  ↪ CINES team (long time storage)
  ↪ Visualisation with SDvision (IRFU/DSM)

Some exascale bottlenecks for GYSELA

- Increase of number of cores ⇒ Hardware/Software failures more frequent

  ➠ Post-Doc ANR-Nufuse G8@Exascale: *O. Thomine (oct 2011-oct 2013)*

  ↪ Fault tolerance improvement

  ↪ Non-blocking writing of restart files *[O. Thomine et al., ESAIM proceedings 2013]*

- BlueGene Architecture fits some of the foreseen requirements for Exascale

  ➠ Post-Doc MDS/PRACE: *J. Bigot (july 2012-july 2014)*

  ↪ Adapting the code for BlueGene architecture

  [J. Bigot, F. Rozar al., ESAIM proceedings 2013]

- Memory reduction per nodes:

  ➠ PhD Maison De la Simulation / IRFM: *F. Rozar (dec 2012-dec 2015)*

  ↪ Development of dedicated tools to improve memory scalability

  [F. Rozar et al., accepted to PPAM2013]

- Big data ∼ Several hundred TBytes: Question of transfer, storage, visualisation

  ↪ HLST support (IPP Garching) for data compression and parallel writting

  ↪ CINES team (long time storage)

  ↪ Visualisation with SDvision (IRFU/DSM)

- Strong efforts of parallelisation since 2009
- Maximum of Gd Challenge opportunities taken to improve GYSELA efficiency

	Relative efficiency		Number of cores
	Strong scaling	Weak scaling	
Gd Challenge CINES (march 2010)	92 %	82 %	8192
Gd Challenge CURIE (march 2012)	91 %	61 %	65 536
Porting on Blue Gene Architecture => Communication schemes rewritten			
Gd Challenge TURING (january 2013)	92 %	61 %	65 536
Access to totality of JUQUEEN (may 2013)		91 %	458 752

x56

↪ Weak scaling: Relative efficiency of 91% on 458 752 cores on the totality of the biggest european machine

WEAK scaling: (on JUQUEEN - Juelich)
Relative efficiency of 91% on 458 752 cores

- Parallel communication schemes completely rewritten
- Tests performed on the totality of JUQUEEN/Blue Gene machine (Juelich)

Execution time, one Gysela (Weak Scaling - Juqueen)

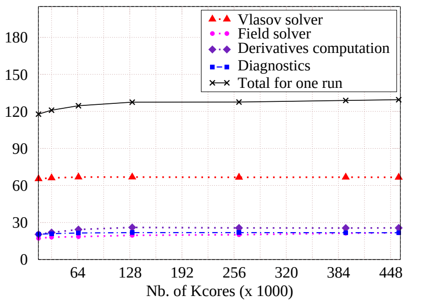

Relative efficiency, one run (Weak scaling - Juqueen)

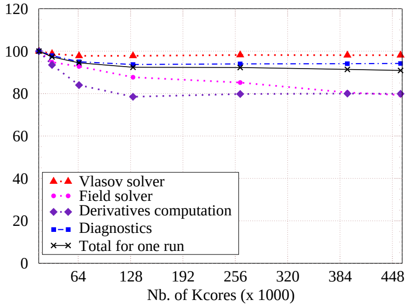

- Weak scaling: Relative efficiency of 91% on 458 752 cores.
  - PRACE preparatory access *(April 2012 - Nov 2012)*: 250 000 hours
  - ANR G8-Exascale via P. Gibbon *(JSC, Juelich, Germany)*.

Improvement of memory consumption

- GYSELA is global ➠ Huge meshes ➠ Constrained by memory per node
- Development of the MTM library in progress (Modelization & Tracing Memory consumption)
  - Identification of memory peak
  - Prediction of memory required before submit ➠ Avoid memory exhaust

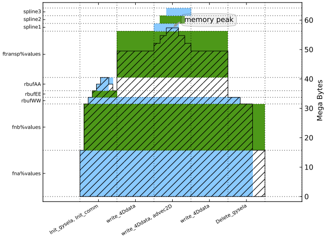

Before optimisation

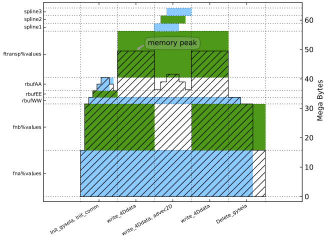

After optimisation

- Static to dynamic memory alloc. + improvement of algorithms

  ➠ Gain of factor 50% on 32k cores

[F. Rozar et al., accepted to PPAM2013]

Lossy Compression for Huge 3D Data (LHCD)

- Problem of memory and time scalability for GYSELA 3D diagnostics
- Development of the LCHD library performed by HLST-IPP Garching
  - 6 months project - S. Espinoza & M. Haefele *[S. Espinoza, HLST Report 2013]*
  - Fast multi-file multi-variable exportation
  - Lossless and lossy 3D data compression

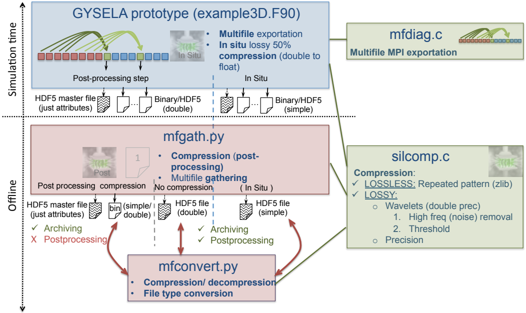

- I/O bandwidth ×26 with parallel efficiency of 95% from 256 to 1280 cores
- Lossless: 8% compression;
- Lossy: from 50% to 70% achieved without altering physics

Outline

1. GYSELA code
2. What challenges for Exascale ?
3. What challenges in terms of numeric ?
   - Modifications of the numerical scheme to improve mass and energy conservation.

Numerical work in progress for WEST/ITER magnetic configurations

geometry

mesh
(equidistant in (r,θ,φ))

magnetic configuration
(simplified circular concentric)

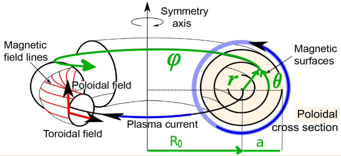

Vlasov

5D Vlasov solver for D + W
(semi-lagrangian scheme)

+ **adiabatic electrons**

$$B_{\|s}^{*}\frac{\partial \bar{F}_s}{\partial t} + \nabla\cdot\left(\frac{d\mathbf{x_G}}{dt}B_{\|s}^{*}\bar{F}_s\right) + \frac{\partial}{\partial v_{G\|}}\left(\frac{dv_{G\|}}{dt}B_{\|s}^{*}\bar{F}_s\right) = C(\bar{F}_s) + S + \mathcal{K}_{\rm buff}(\bar{F}_s) + \mathcal{D}_{\rm buff}(\bar{F}_s)$$

with the equations of motion:

$$B_{\|s}^{*} d_t\mathbf{x}_G = v_{G\|}\mathbf{B}^{*} + \frac{1}{e}\mathbf{b}\times\nabla\Lambda$$

$$B_{\|s}^{*} m_s d_t v_{G\|} = -\mathbf{B}^{*}\cdot\nabla\Lambda$$

J_0 = gyroaverage
(Padé approximation)

where $\mathbf{B}^{*} = \mathbf{B} + (m_s v_{G\|}/e)\nabla\times\mathbf{b}$ and $\Lambda = eJ_0\phi + \mu B$;

Poisson

3D Poisson solver (Finite Differences in r + Fourier in (θ,φ))

$$\frac{e}{T_{e,\rm eq}}\left(\phi - \langle\phi\rangle\right) - \frac{1}{n_{e_0}}\sum_s Z_s \nabla_\perp\cdot\left(\frac{n_{s,\rm eq}}{B\Omega_s}\nabla_\perp\phi\right) = \frac{1}{n_{e_0}}\sum_s Z_s\int J_0\cdot\left(\bar{F}_s - \bar{F}_{s,\rm eq}\right)d^3v$$

Numerical work in progress for WEST/ITER magnetic configurations

geometry

GYSELA poloidal cross-section

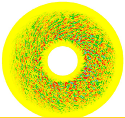

NURBS or Bezier mapping

- complex shapes accessibles
- avoid the hole in the center

Joined effort with JOREK

A. Ratnani (Post-Doc/ANR ANEMOS)

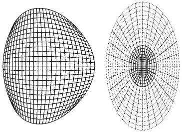

Vlasov

5D Vlasov solver for D + W
(semi-lagrangian scheme)

+ adiabatic electrons

$$B^*_{\parallel s}\frac{\partial \bar{F}_s}{\partial t} + \nabla\cdot\left(\frac{d\mathbf{x_G}}{dt}B^*_{\parallel s}\bar{F}_s\right) + \frac{\partial}{\partial v_{G\parallel}}\left(\frac{dv_{G\parallel}}{dt}B^*_{\parallel s}\bar{F}_s\right) = C(\bar{F}_s) + S + \mathcal{K}_{\rm buff}(\bar{F}_s) + \mathcal{D}_{\rm buff}(\bar{F}_s)$$

with the equations of motion:

$$B^*_{\parallel s} d_t \mathbf{x}_G = v_{G\parallel}\mathbf{B}^* + \frac{1}{e}\mathbf{b}\times\nabla\Lambda$$

$$B^*_{\parallel s} m_s d_t v_{G\parallel} = -\mathbf{B}^*\cdot\nabla\Lambda$$

J_0 = gyroaverage
(Padé approximation)

where $\mathbf{B}^* = \mathbf{B} + (m_s v_{G\parallel}/e)\nabla\times\mathbf{b}$ and $\Lambda = eJ_0\phi + \mu B$;

Poisson

3D Poisson solver (Finite Differences in r + Fourier in (θ,φ))

$$\frac{e}{T_{e,\rm eq}}\left(\phi - \langle\phi\rangle\right) - \frac{1}{n_{e_0}}\sum_s Z_s \nabla_\perp\cdot\left(\frac{n_{s,\rm eq}}{B\Omega_s}\nabla_\perp\phi\right) = \frac{1}{n_{e_0}}\sum_s Z_s\int J_0\cdot\left(\bar{F}_s - \bar{F}_{s,\rm eq}\right)d^3v$$

Numerical work in progress for WEST/ITER magnetic configurations

geometry

GYSELA poloidal cross-section

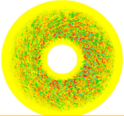

NURBS or Bezier mapping

- complex shapes accessibles
- avoid the hole in the center

Joined effort with JOREK

A. Ratnani (Post-Doc/ANR ANEMOS)

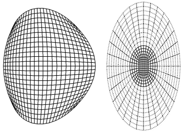

D-shape aligned to B

Vlasov

5D Vlasov solver for D + W (semi-lagrangian scheme) + adiabatic electrons

$$B^*_{\|s}\frac{\partial \bar{F}_s}{\partial t} + \nabla\cdot\left(\frac{d\mathbf{x}_G}{dt}B^*_{\|s}\bar{F}_s\right) + \frac{\partial}{\partial v_{G\|}}\left(\frac{dv_{G\|}}{dt}B^*_{\|s}\bar{F}_s\right) = C(\bar{F}_s) + S + \mathcal{K}_{\mathrm{buff}}(\bar{F}_s) + \mathcal{D}_{\mathrm{buff}}(\bar{F}_s)$$

with the equations of motion:

$$B^*_{\|s} d_t \mathbf{x}_G = v_{G\|}\mathbf{B}^* + \frac{1}{e}\mathbf{b}\times\nabla\Lambda$$

$$B^*_{\|s} m_s d_t v_{G\|} = -\mathbf{B}^*\cdot\nabla\Lambda$$

J_0 = gyroaverage (Padé approximation)

where $\mathbf{B}^* = \mathbf{B} + (m_s v_{G\|}/e)\nabla\times\mathbf{b}$ and $\Lambda = eJ_0\phi + \mu B$;

Poisson

Development of a Poisson solver in generalized coordinates

- collaboration with INRIA : ADT SELALIB

+ A. Back (Post-Doc / ANR GYPSI marseille)

Numerical work in progress for WEST/ITER magnetic configurations

geometry

GYSELA poloidal cross-section

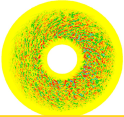

NURBS or Bezier mapping

- complex shapes accessibles
- avoid the hole in the center

Joined effort with JOREK

A. Ratnani (Post-Doc/ANR ANEMOS)

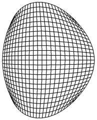

D-shape

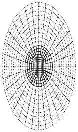

aligned to B

Vlasov

Development of a Vlasov solver on NURBS multipatchs

- collaboration with IPP Garching : *E. Sonnendrücker team*

L. Mendoza (PhD IPP- IRFM joint supervision)

- collaboration with Strasbourg university : *M. Mehrenberger*

+ A. Back (Post-Doc / ANR GYPSI marseille)

Poisson

Development of a Poisson solver in generalized coordinates

- collaboration with INRIA : ADT SELALIB

+ A. Back (Post-Doc / ANR GYPSI marseille)

- Time evolution of gyrocenter distribution function for s species $\bar{F}_s(r,\theta,\varphi,v_\parallel,\mu)$ governed by 5D gyrokinetic Fokker-Planck equation:

[Brizard & Hahm, Rev.Mod.Phys. 2007]

$$B_\parallel^* \frac{\partial \bar{F}_s}{\partial t} + \nabla \cdot \left(\frac{d\mathbf{x_G}}{dt} B_\parallel^* \bar{F}_s \right) + \frac{\partial}{\partial v_{G\parallel}} \left(\frac{dv_{G\parallel}}{dt} B_\parallel^* \bar{F}_s \right) = \mathcal{C}(\bar{F}_s) + S + \mathcal{K}_{\text{buff}}(\bar{F}_s) + \mathcal{D}_{\text{buff}}(\bar{F}_s)$$

with the equations of motion:

$$B_\parallel^* d_t \mathbf{x}_G = v_{G\parallel} \mathbf{B}^* + \frac{1}{e} \mathbf{b} \times \nabla \Lambda$$

$$B_\parallel^* m_s d_t v_{G\parallel} = -\mathbf{B}^* \cdot \nabla \Lambda$$

where

- $\mathbf{B}^* = \mathbf{B} + (m_s v_{G\parallel}/e) \nabla \times \mathbf{b}$ with $\mathbf{b} = \mathbf{B}/B$
- $B_\parallel^* = \mathbf{B}^* \cdot \mathbf{b}$ volume element in guiding-center velocity space
- $\Lambda = \mu B + e \underbrace{J_0 \phi}$

$\phi(\mathbf{x}_G)$: 3D electric potential

J_0: gyroaverage operator $\rightarrow$ Padé approximation

GYSELA - 5D Boltzmann equation

- Time evolution of gyrocenter distribution function for s species $\bar{F}_s(r, \theta, \varphi, v_\parallel, \mu)$ governed by 5D gyrokinetic Fokker-Planck equation:

[Brizard & Hahm, Rev.Mod.Phys. 2007]

$$B_\parallel^* \frac{\partial \bar{F}_s}{\partial t} + \nabla \cdot \left(\frac{d\mathbf{x_G}}{dt} B_\parallel^* \bar{F}_s \right) + \frac{\partial}{\partial v_{G\parallel}} \left(\frac{dv_{G\parallel}}{dt} B_\parallel^* \bar{F}_s \right) = \mathcal{C}(\bar{F}_s) + S + \mathcal{K}_{\rm buff}(\bar{F}_s) + \mathcal{D}_{\rm buff}(\bar{F}_s)$$

- Operators in velocity space:
  - $\mathcal{C}(\bar{F}_s)$ = collision operator
  - S = additional sources
- Operators in buffer regions
  - $\mathcal{K}_{\rm buff}(\bar{F}_s)$ = Krook operator
  - $\mathcal{D}_{\rm buff}(\bar{F}_s)$ = radial diffusion term

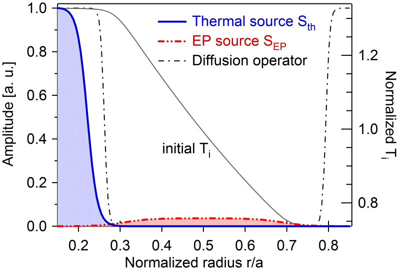

- Time evolution of gyrocenter distribution function for s species $\bar{F}_s(r, \theta, \varphi, v_\parallel, \mu)$ governed by 5D gyrokinetic Fokker-Planck equation:

$$B_\parallel^* \frac{\partial \bar{F}_s}{\partial t} + \nabla \cdot \left(\frac{d\mathbf{x_G}}{dt} B_\parallel^* \bar{F}_s \right) + \frac{\partial}{\partial v_{G\parallel}} \left(\frac{dv_{G\parallel}}{dt} B_\parallel^* \bar{F}_s \right) = \mathcal{C}(\bar{F}_s) + S + \mathcal{K}_{\rm buff}(\bar{F}_s) + \mathcal{D}_{\rm buff}(\bar{F}_s)$$

with the equations of motion:

$$B_\parallel^* d_t \mathbf{x}_G = v_{G\parallel} \mathbf{B}^* + \frac{1}{e} \mathbf{b} \times \nabla \Lambda$$

$$B_\parallel^* m_s d_t v_{G\parallel} = -\mathbf{B}^* \cdot \nabla \Lambda$$

where $\mathbf{B}^* = \mathbf{B} + (m_s v_{G\parallel}/e) \nabla \times \mathbf{b}$ and $\Lambda = e J_0 \phi + \mu B$;

- Self-consistency ensured by a 3D quasi-neutrality equation:

$$\frac{e}{T_{e,\rm eq}} \left(\phi - \langle \phi \rangle \right) - \frac{1}{n_{e_0}} \sum_s Z_s \nabla_\perp \cdot \left(\frac{n_{s,\rm eq}}{B \Omega_s} \nabla_\perp \phi \right) = \frac{1}{n_{e_0}} \sum_s Z_s \int J_0 \cdot \left(\bar{F}_s - \bar{F}_{s,\rm eq} \right) d^3 v$$

Actual time-splitting for Vlasov ($\tilde{\mathcal{V}}$)

- A time-splitting of Strang is applied to the Vlasov equation:

$$B_{\parallel}^{*}\frac{\partial \bar{F}_s}{\partial t} + \nabla\cdot\left(\frac{d\mathbf{x_G}}{dt}B_{\parallel}^{*}\bar{F}_s\right) + \frac{\partial}{\partial v_{G\parallel}}\left(\frac{dv_{G\parallel}}{dt}B_{\parallel}^{*}\bar{F}_s\right) = 0$$

- Let us define three operators (with $\mathcal{X}_G = (r,\theta)$)

$$B_{\parallel s}^{*}\frac{\partial \bar{F}_s}{\partial t} + \boldsymbol{\nabla}\cdot\left(B_{\parallel s}^{*}\frac{\mathrm{d}\mathcal{X}_G}{\mathrm{d}t}\bar{F}_s\right) = 0 \qquad : (\tilde{\mathcal{X}}_G) \quad \leftarrow \quad 2D$$

$$B_{\parallel s}^{*}\frac{\partial \bar{F}_s}{\partial t} + \frac{\partial}{\partial \varphi}\left(B_{\parallel s}^{*}\frac{\mathrm{d}\varphi}{\mathrm{d}t}\bar{F}_s\right) = 0 \qquad : (\tilde{\varphi}) \quad \leftarrow \quad 1D$$

$$B_{\parallel s}^{*}\frac{\partial \bar{F}_s}{\partial t} + \frac{\partial}{\partial v_{G\parallel}}\left(B_{\parallel s}^{*}\frac{\mathrm{d}v_{G\parallel}}{\mathrm{d}t}\bar{F}_s\right) = 0 \qquad : (\tilde{v_{G\parallel}}) \quad \leftarrow \quad 1D$$

- Then, a Vlasov solving sequence ($\tilde{\mathcal{V}}$) is performed as:

$$(\tilde{\mathcal{V}}) \equiv \left(\frac{\tilde{v_{G\parallel}}}{2}, \frac{\tilde{\varphi}}{2}, \tilde{\mathcal{X}}_G, \frac{\tilde{\varphi}}{2}, \frac{\tilde{v_{G\parallel}}}{2}\right)$$

- At each step: 1 advection and 1 interpolation per grid point (by cubic splines).

Splitting into linear and non-linear parts (1/2)

$$\frac{\mathrm{d}x_G^i}{\mathrm{d}t} = v_{G\|}\mathbf{b}_s^* \cdot \nabla x_G^i + \mathbf{v}_{E\times B_s} \cdot \nabla x_G^i + \mathbf{v}_{D_s} \cdot \nabla x_G^i \qquad (1)$$

$$m_s \frac{\mathrm{d}v_{G\|}}{\mathrm{d}t} = -\mu \mathbf{b}_s^* \cdot \nabla B - q_s \mathbf{b}_s^* \cdot \nabla \bar{\phi} + \frac{m_s v_{G\|}}{B} \mathbf{v}_{E\times B_s} \cdot \nabla B \qquad (2)$$

where the *i*-th contravariant coordinates of the drift velocities are given by:

$$\mathbf{v}_{E\times B_s} \cdot \nabla x_G^i = \mathbf{v}_{E\times B_s}^i = \frac{1}{B_{\|s}^*}\left[\bar{\phi}, x_G^i\right] \qquad \textit{(ExB drift)} \qquad (3)$$

and

$$\mathbf{v}_{D_s} \cdot \nabla x_G^i = \mathbf{v}_{D_s}^i = \left(\frac{m_s v_{G\|}^2 + \mu B}{q_s B_{\|s}^* B}\right)\left[B, x_G^i\right] \qquad \textit{(curvature drift)} \qquad (4)$$

$$\frac{dx_G^i}{dt} = v_{G\parallel}\mathbf{b}_s^* \cdot \nabla x_G^i + \mathbf{v}_{E\times B_s} \cdot \nabla x_G^i + \mathbf{v}_{D_s} \cdot \nabla x_G^i \quad (1)$$

$$m_s \frac{dv_{G\parallel}}{dt} = -\mu \mathbf{b}_s^* \cdot \nabla B - q_s \mathbf{b}_s^* \cdot \nabla \bar{\phi} + \frac{m_s v_{G\parallel}}{B} \mathbf{v}_{E\times B_s} \cdot \nabla B \quad (2)$$

where the i-th contravariant coordinates of the drift velocities are given by:

$$\mathbf{v}_{E\times B_s} \cdot \nabla x_G^i = \mathbf{v}_{E\times B_s}^i = \frac{1}{B_{\parallel s}^*}\left[\bar{\phi}, x_G^i\right] \qquad \textit{(ExB drift)} \quad (3)$$

and

$$\mathbf{v}_{D_s} \cdot \nabla x_G^i = \mathbf{v}_{D_s}^i = \left(\frac{m_s v_{G\parallel}^2 + \mu B}{q_s B_{\parallel s}^* B}\right)\left[B, x_G^i\right] \qquad \textit{(curvature drift)} \quad (4)$$

- ☹ Large shifts in (r, θ) and φ at each directional advection at high $v_{G\parallel}$
  - Error of evaluation of electric field at each substep of the splitting
- ➠ Same idea than Y. Idomura *[CPC '08]* ➠ Separate between:
  - linear terms and
  - non-linear terms ➠ depending on the electric potential $\bar{\phi}$.

- Equations (1)-(2) are split into two operators:

Linear operator $\mathcal{L}$

$$\frac{dx_G^i}{dt} = v_{G\parallel}\mathbf{b}_s^* \cdot \nabla x_G^i + \mathbf{v}_{D_s} \cdot \nabla x_G^i$$

$$m_s \frac{dv_{G\parallel}}{dt} = -\mu \mathbf{b}_s^* \cdot \nabla B$$

Nonlinear operator $\mathcal{N}$

$$\frac{dx_G^i}{dt} = \mathbf{v}_{E\times B_s} \cdot \nabla x_G^i$$

$$m_s \frac{dv_{G\parallel}}{dt} = -q_s \mathbf{b}_s^* \cdot \nabla\bar{\phi} + \frac{m_s v_{G\parallel}}{B}\mathbf{v}_{E\times B_s} \cdot \nabla B$$

Splitting into linear and non-linear parts (2/2)

- Equations (1)-(2) are split into two operators:

Linear operator $\mathcal{L}$

$$\frac{dx_G^i}{dt} = v_{G\parallel}\mathbf{b}_s^* \cdot \nabla x_G^i + \mathbf{v}_{D_s} \cdot \nabla x_G^i$$

$$m_s \frac{dv_{G\parallel}}{dt} = -\mu \mathbf{b}_s^* \cdot \nabla B$$

$$\Downarrow$$

large displacements at large $|v_{G\parallel}|$

- Trajectories precomputed in 4D one times at the beginning and saved
  - Runge-Kutta 2 with a small time step

    $\delta t = \Delta t / M$ with $M = 64$
- Cubic spline interpolation in 4D

Nonlinear operator $\mathcal{N}$

$$\frac{dx_G^i}{dt} = \mathbf{v}_{E\times B_s} \cdot \nabla x_G^i$$

$$m_s \frac{dv_{G\parallel}}{dt} = -q_s \mathbf{b}_s^* \cdot \nabla \bar{\phi} + \frac{m_s v_{G\parallel}}{B} \mathbf{v}_{E\times B_s} \cdot \nabla B$$

$$\Downarrow$$

shifts coupled to E field

- Solved as previously on a Δt

➡ Computational time per global iteration nearly $\times 2$ but Δt can be $\nearrow$

$$\mathcal{L}\left(\frac{\tilde{\mathbf{Z}}}{2}\right) \quad \mathcal{N}\left(\frac{\tilde{v_{G\parallel}}}{2}, \frac{\tilde{\varphi}}{2}, \tilde{\mathcal{X}}_G, \frac{\tilde{\varphi}}{2}, \frac{\tilde{v_{G\parallel}}}{2}\right) \quad \mathcal{L}\left(\frac{\tilde{\mathbf{Z}}}{2}\right) \qquad \text{where } \mathbf{Z} = (r, \theta, \varphi, v_{G\parallel})$$

Relevant 4D case for numerical tests ?

☹ Difficult to test numerical schemes on 5D expensive computational simulations

- Work in progress: Definition of relevant cases for numerical tests
  - More relevant than the 4D cylindrical drift-kinetic case proposed in *[Grandgirard, JOCP 2006]* for phenomena appearing in tokamak plasma simulations.
  - Sufficiently small to be run on few cores during few hours.
- Objective: Tractable test cases for SELALIB platform
  - SELALIB a numerical test platform for Vlasov solvers developed at INRIA-Strasbourg. *[E. Chacon-Golcher, P. Navaro]*

Relevant 4D case for numerical tests ?

☹ Difficult to test numerical schemes on 5D expensive computational simulations

- Work in progress: Definition of relevant cases for numerical tests
  - More relevant than the 4D cylindrical drift-kinetic case proposed in *[Grandgirard, JOCP 2006]* for phenomena appearing in tokamak plasma simulations.
  - Sufficiently small to be run on few cores during few hours.
- Objective: Tractable test cases for SELALIB platform
  - SELALIB a numerical test platform for Vlasov solvers developed at INRIA-Strasbourg. *[E. Chacon-Golcher, P. Navaro]*

$\Downarrow$

- A 4D gyrokinetic toroidal case (i.e $(r, \theta, \varphi, v_{G\parallel})$ with $\mu \neq 0$) takes into account
  - The curvature of the magnetic field lines *(i.e not cylindrical)*
  - The gyroaverage operator ($J_0 = \mathrm{I}_d$ for $\mu = 0$) *(i.e not drift-kinetic)*
  - Motion in $v_{G\parallel}$ for the unperturbed trajectories ($\mathrm{d}v_{G\parallel}/\mathrm{d}t = 0$ for $\mu = 0$).

➠ Case for results presented in the following
  - $\rho_* = 1/75$; Domain discretization: $N_r = 128$, $N_\theta = 128$, $N_\varphi = 64$, $N_{v_\parallel} = 92$
  - 256 cores during $\sim$ 12 hours

Drift-kinetic cases necessary but not sufficient for test of numerical schemes (1/2)?

- Rk: In the following BSL refers to the scheme currently used in GYSELA
- BSL ➠ L1-norm and energy well conserved in drift-kinetic 4D case (i.e $\mu = 0$)

  [Latu, Grandgirard et al.,RR8054-INRIA 2012]

  - Relative error of 10^{-6} on L1-norm

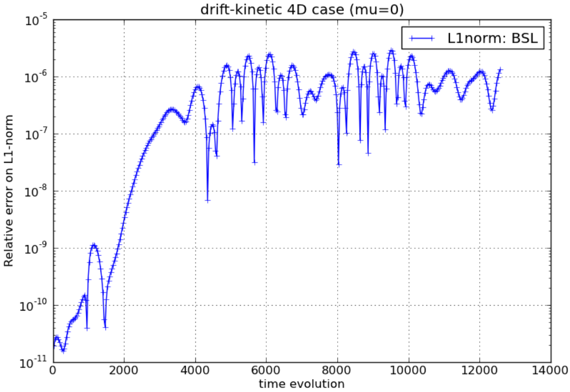

Drift-kinetic cases necessary but not sufficient for test of numerical schemes (1/2)?

- Rk: In the following BSL refers to the scheme currently used in GYSELA
- BSL ➠ L1-norm and energy well conserved in drift-kinetic 4D case (i.e $\mu = 0$)
  [Latu, Grandgirard et al.,RR8054-INRIA 2012]
  - Relative error on total energy conservation of few %

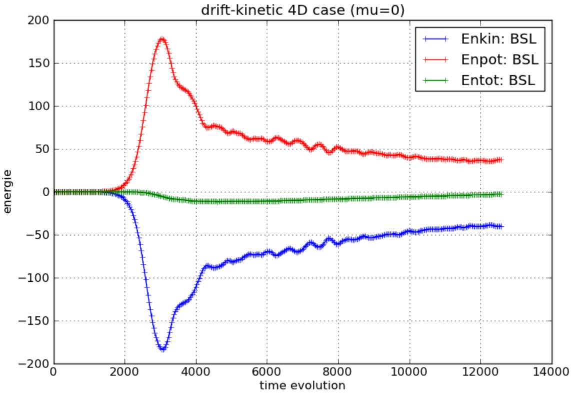

Drift-kinetic cases necessary but not sufficient for test of numerical schemes (2/2)?

- BSL ➠ Not exactly the same story for a gyrokinetic 4D case (i.e $\mu \neq 0$)
  - Relative error on L1-norm of 10^{-5} compared to 10^{-6} for drift-kinetic case

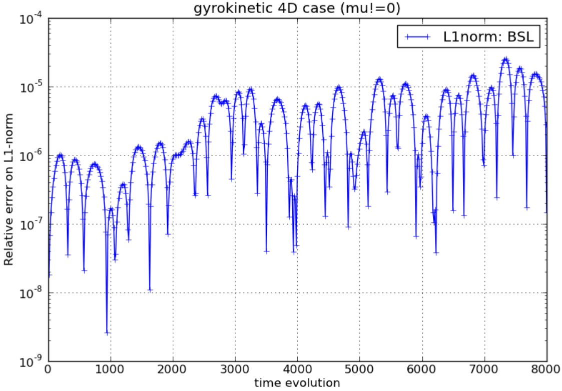

➠ Gyrokinetic 4D case is more constraining than drift-kinetic 4D case

Drift-kinetic cases necessary but not sufficient for test of numerical schemes (2/2)?

- BSL ➠ Not exactly the same story for a gyrokinetic 4D case (i.e $\mu \neq 0$)
  - Relative error on L1-norm of 10^{-5} compared to 10^{-6} for drift-kinetic case
  - Degradation of the total energy conservation

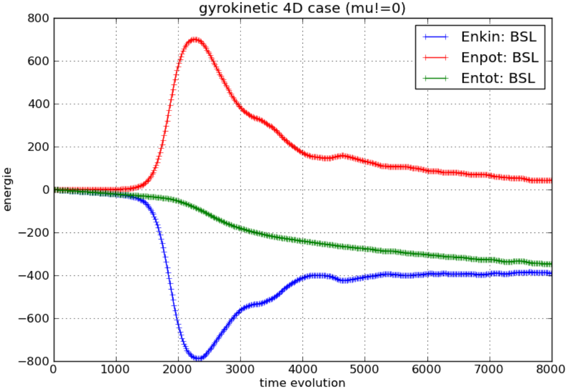

➠ Gyrokinetic 4D case is more constraining than drift-kinetic 4D case

Improvement with linear/non-linear splitting

- Rk: In the following BSL-(L/NL) refers to the scheme with linear/non-linear splitting.
- Comparison between BSL and BSL-(L/NL) schemes for gyrokinetic 4D cases
  - Relative error on L1-norm not changed

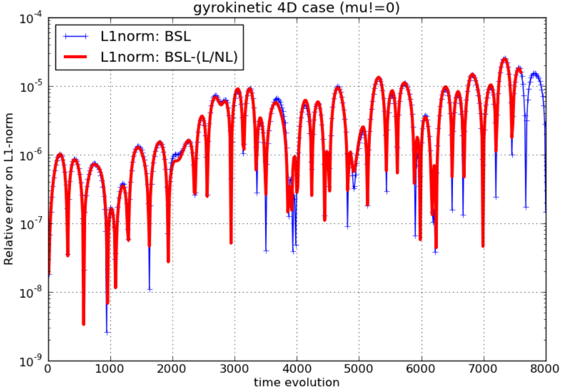

Improvement with linear/non-linear splitting

- Rk: In the following BSL-(L/NL) refers to the scheme with linear/non-linear splitting.
- Comparison between BSL and BSL-(L/NL) schemes for gyrokinetic 4D cases
  - Relative error on L1-norm not changed
  - But significant improvement of energy conservation

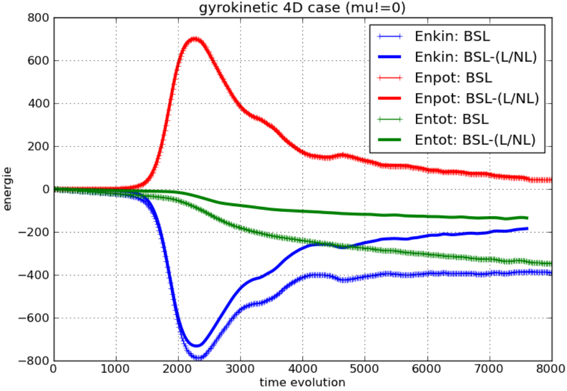

New improvement: δF on the linear part

- In a full-*f* code as GYSELA the distribution function is initialized as

$$F = F_{\mathrm{eq}} + \delta F \quad \text{with } F_{\mathrm{eq}} \text{ equilibrium function and } \delta F \text{ perturbation}$$

- Idea: Any function of constants of motion in the unperturbed characteristics is an equilibrium of the collisionless gyrokinetic equation.

  ➡ Use the fact that any function of the motion invariants is invariant by the linear operator $\mathcal{L}(\tilde{\mathbf{Z}})$

- New algorithm for the 4D linear splitting:
  - Initialization of F_{eq} as a function of the motion invariants
  - For each time iteration between t^n and t^{n+1}:
    1. $\delta F^n = F^n - F_{\mathrm{eq}}$
    2. $\delta F^{n+1} = \mathcal{L}(\delta F^n)$ ← linear 4D advection
    3. $F^{n+1} = \delta F^{n+1} + F_{\mathrm{eq}}$

- Objective: Use the fact that 4D interpolation of δF should be better than on F

- In an axisymmetric toroidal configuration a GK vlasov equilibrium is defined by three constants of motion:
  - the magnetic momentum μ,
  - the energy $\mathcal{E} = m_s v_{G\parallel}^2/2 + \mu B(r,\theta)$ and
  - the canonical toroidal angular momentum $P_\varphi = \psi(r) + I v_{G\parallel}/B(r,\theta)$ where $\psi(r)$ defined by $\mathrm{d}\psi/\mathrm{d}r = -B_0 r/q(r)$ with $q(r)$ the safety factor.

➠ Finding $F_{\rm eq}$ as a function of the invariants $(\mu, \mathcal{E}, P_\varphi)$ with the two following physical constraints is not trivial at all
  - $n(r) = \int F_{\rm eq}\, \mathrm{d}\theta\, \mathrm{d}\varphi\, \mathrm{d}v_{G\parallel}$ close to physical radial density profile
  - $T(r) = \int F_{\rm eq} \mathcal{E}\, \mathrm{d}\theta\, \mathrm{d}\varphi\, \mathrm{d}v_{G\parallel}/n(r)$ close to physical radial temperature profile

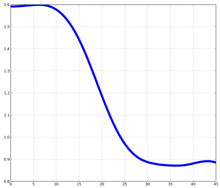

radial density profile

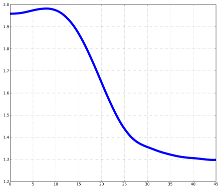

radial temperature profile

δF on the linear part improves conservation

- Rk: In the following BSL-(L/NL)-deltaF refers to the scheme with linear/non-linear splitting and with δF interpolation.
- Comparison between BSL-(L/NL) and BSL-(L/NL)-deltaF schemes for gyrokinetic 4D cases
  - Significant improvement on L1-norm during the linear phase

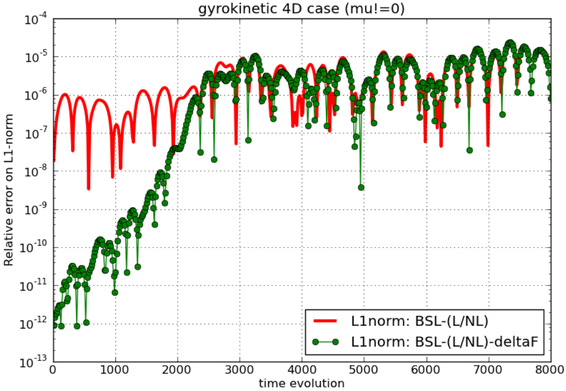

δF on the linear part improves conservation

- Rk: In the following BSL-(L/NL)-deltaF refers to the scheme with linear/non-linear splitting and with δF interpolation.
- Comparison between BSL-(L/NL) and BSL-(L/NL)-deltaF schemes for gyrokinetic 4D cases
  - Significant improvement on L1-norm during the linear phase
  - Small improvement of energy conservation

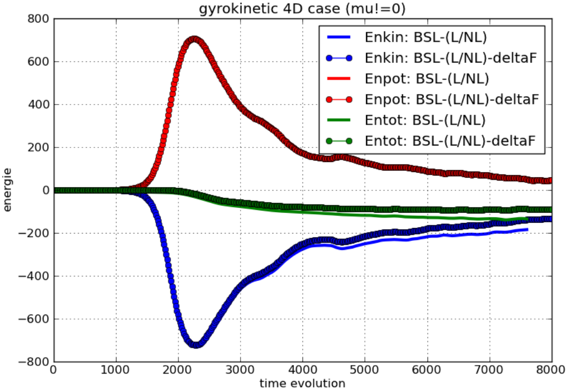

What is the impact of conservation on physical results?

- Impact of the different L1-norm and energy conservation is not significant on physical results as temperature, pressure, turbulent heat flux, etc..

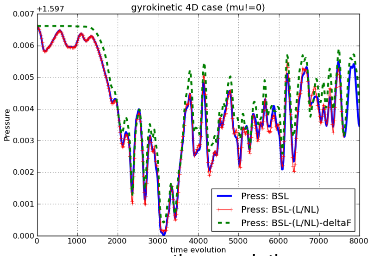

pressure time evolution

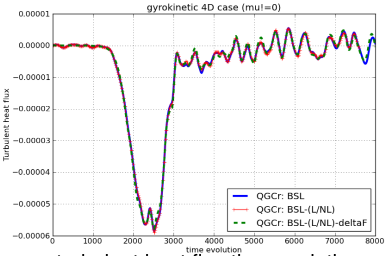

turbulent heat flux time evolution

- An impact could appear for long time simulations
- Even with standard BSL scheme GYSELA code has shown
  - An accurate description of the radial force balance *[Dif-Pradalier, PoP 2011]*
  - An accurate conservation of the toroidal angular momentum *[Abiteboul, PoP 2011]*

⇒ Which impact of non-conservation of L1-norm and energy on physical results ?

Conclusion - Perspectives

- Each GYSELA simulation = a numerical experiments
  ↪ Several weeks on several thousands of core
  (ex: Grand Challenge Curie 2012: 15 days on 16384 cores)
  ↪ Several TBytes of data to store and to analyse
- Exascale HPC will be required for realistic simulation with both ions and kinetic electrons
  ↪ Promising results: Weak scaling - relative efficiency of 91% on 458 752 cores
- Not trivial to define test cases with complexity close to realistic cases but tractable for numerical tests
  - Drift-kinetic 4D case necessary but not sufficient
  - ➠ Gyrokinetic 4D test case most constraining
- The semi-lagrangian scheme can been improved in the GYSELA code
  - by using an linear/non-linear splitting
  - by interpolating on δF instead of F

Collaborations:

- ANR GYPSI (2010-2014)
  ↪ Strasbourg, Nancy, Marseille
- ANR Nufuse G8@exascale (2012-2016)
  ↪ France, Germany, Japan, US, UK
- ADT INRIA Selalib (2011-2015)
  ↪ Strasbourg, Bordeaux
- IPL INRIA (march 2013-2017)
  ↪ Nice, Bordeaux
- New project following AEN INRIA Fusion (evaluation in progress)
  ↪ Strasbourg, Lyon, Nice
- Collaborations with IPP Garching (Germany) since 2012
- Collaborations with “Maison de la Simulation”- Saclay (Paris) since 2012

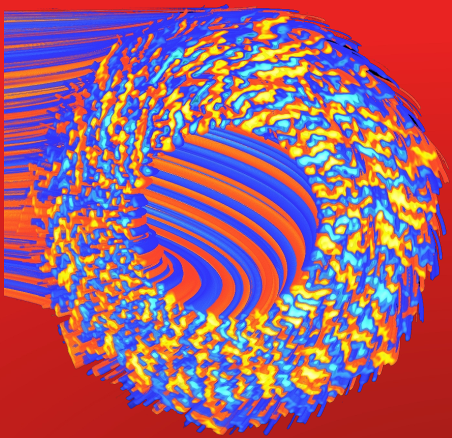

Commissariat à l'énergie atomique et aux énergies alternatives
Centre de Cadarache | 13108 Saint Paul Lez Durance Cedex
T. +33 (0)4 42 25 46 59 | F. +33 (0)4 42 25 64 21

DSM
IRFM
SCCP/GTTM